

FIG. 1: Optical (a) and SEM (b) images of a nested trampoline resonator. The device was broken out of the chip to make the structure visible for (b). Note the thin 10 μm wide, 500 nm thick arms supporting the large 500 μm thick silicon mass. A properly sized mirror layer was necessary to protect the nitride layer from sharp edges in the silicon and safely connect to the thin arms of the outer resonator. (c) A schematic overview of the fabrication process (not to scale). (i) The SiO<sub>2</sub>/Ta<sub>2</sub>O<sub>5</sub> DBR stack is etched via CHF<sub>3</sub> ICP etch. The front (ii) and back (iii) Si<sub>3</sub>N<sub>4</sub> is etched by CF<sub>4</sub> plasma etch. (iv) Most of the Si is etched from the bottom using the Bosch process. (v) The remainder of the Si is etched via TMAH. (vi) A buffered HF dip cleans the devices and removes a protective SiO<sub>2</sub> layer. Only 6 layers of the SiO<sub>2</sub>/Ta<sub>2</sub>O<sub>5</sub> DBR stack are shown, and the shape of the outer resonator mass is approximated as a hollow cylinder for simplicity.

Devices are fabricated starting with a superpolished 500 micron thick silicon wafer. Either 300 or 500 nm of high stress LPCVD Si<sub>3</sub>N<sub>4</sub> is deposited on both sides of the wafer, and a commercially procured SiO<sub>2</sub>/Ta<sub>2</sub>O<sub>5</sub> DBR is deposited on top. The DBR is etched into a small mirror on the inner resonator and a protective mirror layer on the outer resonator using a CHF<sub>3</sub> inductively coupled plasma (ICP) etch. Next, the Si<sub>3</sub>N<sub>4</sub> arms of the devices are patterned with a CF<sub>4</sub> etch. A window is also opened on the back side Si<sub>3</sub>N<sub>4</sub> with a CF<sub>4</sub> etch. Approximately 400 microns of silicon under the Si<sub>3</sub>N<sub>4</sub> arms are removed from the back using the Bosch deep reactive ion etch process. A large silicon mass is left in place between the inner and outer arms of the device. The devices are then released with a tetramethylammonium hydroxide (TMAH) etch. Finally a buffered HF etch removes the top protective buffer layer of SiO<sub>2</sub> without damaging the underlying Ta<sub>2</sub>O<sub>5</sub> layer. Figure 1 shows a schematic summary of the fabrication process.

Devices are characterized using a 1064 nm NdYAG laser. To measure mechanical motion, the Fabry-Pérot cavity is first intentionally misaligned to a finesse of around 100 to avoid any optomechanical effects. The cavity is then locked to the laser frequency at the inflection point of a Fabry-Pérot fringe using a piezoelectric actuator moving the position of the large mirror. Quality factors are taken from Lorentzian fits to the power

spectral density of the Brownian motion of the devices. Finesse is measured by optical ringdown [26].

As an initial step, a series of single trampoline resonators with 60 μm diameter mirrors and varying geometries were fabricated and the mechanical quality factors measured [29, 30]. Three of the devices are pictured in Figure 2. We observed no significant geometric trends in quality factor. However, we found that remounting the same sample can change the quality factor of the devices by more than a factor of 10. Table I shows the quality factors for the devices on one chip mounted three separate times. It is clear that mounting drastically affects the quality factor; we attribute this to a change in the clamping loss, because we observe mechanical modes in the system around the resonance frequency that change in number, frequency and power with mounting. Clamping loss can be modeled as a coupling to these external mechanical modes [14, 31].

We now turn to the nested trampoline resonators (see Figure 1.) The outer resonator acts as a low pass filter, providing 40 dB of isolation for every decade of frequency difference between the inner and the outer resonator (see Equation 1.) To test the mechanical isolation we performed a vibration transmission experiment. We attached a ring piezo to the sample mount with springs and applied a sinusoidal signal of varying frequency to the piezo. We measured the motion of the chip using

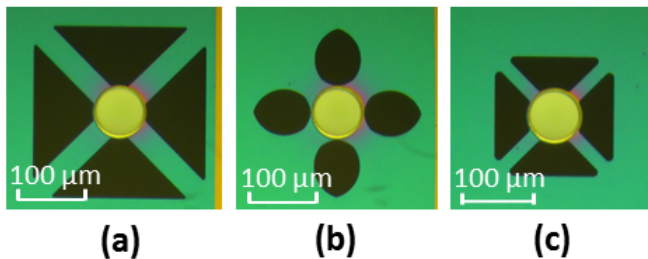


FIG. 2: Optical microscope images of three single resonator devices. A number of different geometries were fabricated with different arm length, arm width and fillet size.

Mounting	Device a	Device b	Device c
1	$425,000 \pm 32,000$	$80,000 \pm 4,000$	$33,000 \pm 2,000$
2	$38,000 \pm 2,000$	$5,000 \pm 1,000$	$40,000 \pm 2,000$
3	$264,000 \pm 21,000$	$16,000 \pm 1,000$	$113,000 \pm 8,000$

TABLE I: This table shows the quality factors for the three devices pictured in Figure 2 with three different mountings. The importance of clamping loss is evident from the changes in quality factor of more than a factor of ten based on the mounting.

a Michelson interferometer and the motion of the inner mirror using a low finesse Fabry-Pérot cavity as described above. The ratio of these two signals is the mechanical transmission from the chip mounting to the inner mirror.

This challenging experiment required eight orders of magnitude to be measured in the same frequency scan. Because of insufficient laser scanning range, the Michelson interferometer was uncalibrated and the DC response was used for calibration. Due to the requirement for a single scan, measurement averaging time was limited by drift in the interferometer. The mechanical response of the piezo also dropped off significantly after 100 kHz, so it was not possible to measure the mechanical transmission at the frequency of the inner resonator. Figure 3 shows the transmission for both a single and a nested resonator. The data are binned for clarity, with the error bars reflecting variations within each bin. The experimental data follow the trend predicted by Equation 1 quite well. The theory curve is not a fit;  $\omega_o$  and  $\gamma_o$  were determined through independent measurements. The deviations at high frequency are likely due to insufficient signal to noise ratio. The results clearly indicate that the outer resonator provides approximately 40 dB per decade of mechanical isolation. We can only measure a maximum of 45 dB of isolation, but we would expect 80 dB of isolation if we continued the measurement up to the inner resonator frequency.

We also tested the mounting dependence of the quality factor. The results of remounting a single nested resonator five times are shown in Table II. The quality factor of the outer resonator changes drastically between the mountings, indicating that the mechanical clamping loss is changing. However, the inner resonator only demon-

Mounting	Inner Resonator Q	Outer Resonator Q
1	$418,000 \pm 11,000$	$700,000 \pm 100,000$
2	$427,000 \pm 10,000$	$690,000 \pm 100,000$
3	$481,000 \pm 12,000$	$70,000 \pm 20,000$
4	$462,000 \pm 14,000$	$240,000 \pm 40,000$
5	$457,000 \pm 13,000$	$220,000 \pm 40,000$

TABLE II: This table shows the quality factors of a nested trampoline resonator remounted five different times. The outer resonator quality factor (measured via ringdown) has large variation between the mountings while the inner resonator quality factor (measured via a fit to thermal motion) has only small variation between the mountings.

strates changes in quality factor on the order of 10%. The relatively small variation in quality factor of the inner resonator and the absence of extra mechanical peaks around the resonance frequency indicate that the clamping loss of the device has largely been eliminated. Indeed, all nested resonators fabricated without any obvious physical defects had quality factors between 300,000 and 500,000. The highest quality factor achieved was  $481,000 \pm 12,000$ , an order of magnitude larger than for comparable silicon devices at room temperature [24]. Typical quality factor measurements for an inner and outer resonator are shown in Figure 4.

One concern for experiments with this system is the thermal motion of the outer resonator (10-100 pm rms at room temperature). Because of the narrow linewidth of the cavity, the optical response to such a large motion is nonlinear. However, the frequency of the outer resonator is low enough that a PID controller can lock a laser to the cavity, tracking the motion and removing any nonlinear effects. In addition, if the laser is locked with a slight negative detuning from the cavity resonance, the outer resonator can be optomechanically cooled, even without being sideband resolved [2]. Thus, the motion of the outer resonator does not prevent experiments using the inner resonator.

Another concern is maintaining the high quality of the DBR mirror layer through the fabrication process. Reducing the optical loss rate is critical to developing a system that allows quantum optical manipulation of mechanical motion. One way to reduce the optical loss rate is through superpolishing the wafer surfaces before deposition of the DBR, to reduce scattering. The addition of this step, as well as the selection of very highly reflective DBR coatings enable us to achieve a Fabry-Pérot cavity with finesse  $181,000 \pm 1,000$ , (optical linewidth 17 kHz) the highest finesse reported in an optomechanical Fabry-Pérot system. The ringdown measurement is shown in Figure 4. All of the nested resonators measured have finesse greater than 160,000, indicating that the nested trampoline fabrication process is completely compatible with maintaining highly reflective mirror surfaces.

Improvements in finesse and mechanics will enable new experiments with trampoline resonators. Our system (using the device in Figure 4) is fourteen times sideband

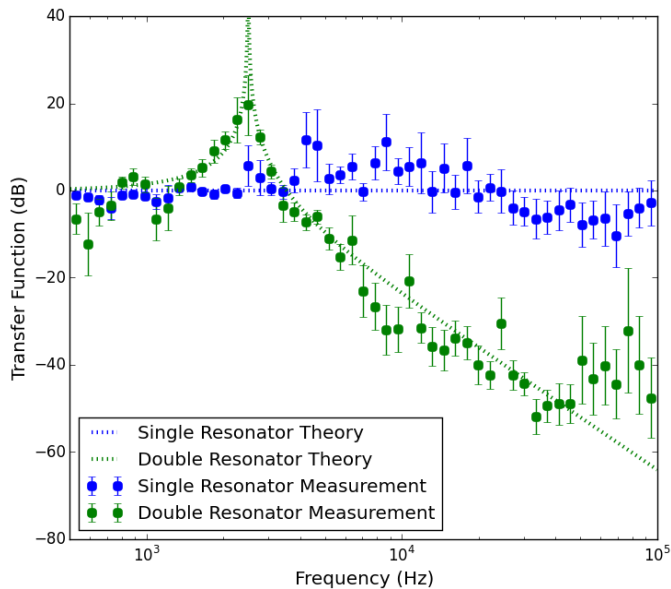


FIG. 3: Transfer function of a single and nested resonator. A sample mount with a single (blue) and nested (green) resonator was mechanically driven at a range of frequencies. The motion of the outer chip and the inner mirror were measured to get the mechanical transfer function. The height at DC frequencies is adjusted to zero. This plot demonstrates that the nested resonator scheme provides mechanical isolation as predicted by Equation 1.

resolved, which is more than sufficient for experiments such as quantum nondemolition measurements [32]. The elimination of the clamping loss will enable another systematic study of the geometry like the one attempted with single resonators. Many mechanical devices using  $\text{Si}_3\text{N}_4$  without a DBR have much higher quality factor [18, 19, 33]. Varying the design of the inner resonator could allow reduction of mirror-nitride loss and fabrication of devices with even higher quality factors.

The improvements in mechanical isolation should also enable optomechanical cooling to the ground state. The devices are shielded from environmental mechanical noise, which previously could obscure motion at the quantum level. The  $fQ$  product of  $1.1 \times 10^{11}$  Hz (for the device from Table II) is also high enough for cooling to the ground state from 4 K, potentially alleviating the need for a dilution refrigerator. Our sideband resolution yields a theoretical minimum of  $3 \times 10^{-4}$  phonons from optical cooling if there is no heating of the system [11]. One concern is the thermal conductivity of our design, because at 4 K the thermal conductivity of  $\text{Si}_3\text{N}_4$  drops to about  $10^{-2}$  W/mK [34, 35]. The heat conduction is limited by the arms of the outer resonator, which are five to fifteen times narrower than the arms of the inner resonator. We have previously thermalized single

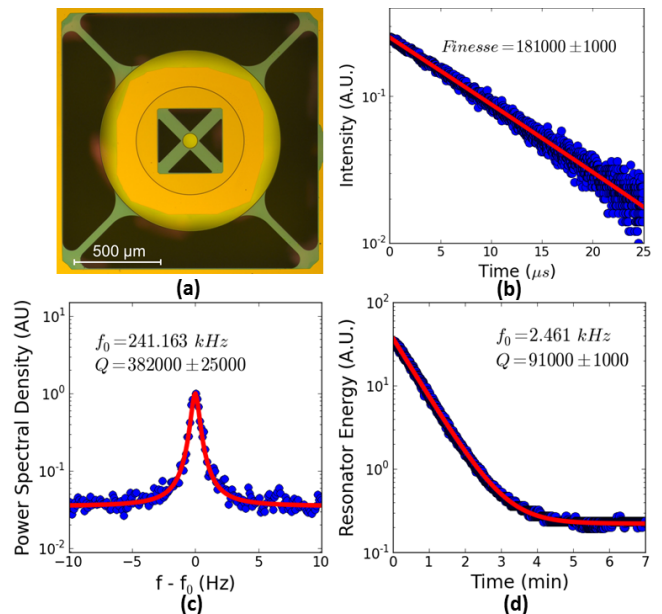


FIG. 4: Measurements of a nested trampoline resonator (the same device as for Figure 3.) (a) Optical microscope image. (b) Optical ringdown to measure the cavity finesse. (c) Lorentzian fit to thermal motion of the inner resonator to measure quality factor. (d) Mechanical ringdown of the outer resonator to measure quality factor taken using a lock-in amplifier.

resonators to 100 mK temperature, so thermalizing a double resonator sample to 4K, even with the narrower arms, should not be a problem.

We have demonstrated that we can consistently fabricate nested trampoline devices with both high quality factor and high finesse. We design the devices to have 80 dB of mechanical isolation from the environment at the inner resonator frequency, and we observe greater than 45 dB of mechanical isolation at lower frequencies and the elimination of clamping losses. These high quality parameters will pave the way to fabrication of even better devices and measurements at low temperatures.

## I. ACKNOWLEDGMENTS

The authors would like to thank H. van der Meer for technical assistance and support and P. Sonin for helpful discussion about the design of single resonators. This work is supported by National Science Foundation Grant No. PHY-1212483. This work is also part of the research program of the Foundation for Fundamental Research on Matter (FOM) and of the NWO VICI research program, which are both part of the Netherlands Organisation for Scientific Research (NWO).

[1] P. Meystre, *Annalen der Physik* **525**, 215 (2013).

[2] M. Aspelmeyer, T. J. Kippenberg, and F. Marquardt,

- Reviews of Modern Physics **86**, 1391 (2014).
- [3] A. D. O’Connell, M. Hofheinz, M. Ansmann, R. C. Bialczak, M. Lenander, E. Lucero, M. Neeley, D. Sank, H. Wang, M. Weides, et al., *Nature* **464**, 697 (2010).
- [4] J. Chan, T. P. M. Alegre, A. H. Safavi-Naeini, J. T. Hill, A. Krause, S. Gröblacher, M. Aspelmeyer, and O. Painter, *Nature* **478**, 89 (2011).
- [5] J. D. Teufel, T. Donner, D. Li, J. W. Harlow, M. S. Allman, K. Cicak, A. J. Sirois, J. D. Whittaker, K. W. Lehnert, and R. W. Simmonds, *Nature* **475**, 359 (2011).
- [6] S. Weis, R. Rivière, S. Deléglise, E. Gavartin, O. Arcizet, A. Schliesser, and T. J. Kippenberg, *Science* **330**, 1520 (2010).
- [7] A. H. Safavi-Naeini, T. P. M. Alegre, J. Chan, M. Eichenfield, M. Winger, Q. Lin, J. T. Hill, D. E. Chang, and O. Painter, *Nature* **472**, 69 (2011).
- [8] J. D. Teufel, D. Li, M. S. Allman, K. Cicak, A. J. Sirois, J. D. Whittaker, and R. W. Simmonds, *Nature* **471**, 204 (2011).
- [9] T. A. Palomaki, J. D. Teufel, R. W. Simmonds, and K. W. Lehnert, *Science* **342**, 710 (2013).
- [10] W. Marshall, C. Simon, R. Penrose, and D. Bouwmeester, *Physical Review Letters* **91**, 130401 (2003).
- [11] F. Marquardt, J. P. Chen, A. A. Clerk, and S. M. Girvin, *Physical Review Letters* **99**, 093902 (2007).
- [12] I. Wilson-Rae, N. Nooshi, W. Zwerger, and T. J. Kippenberg, *Physical Review Letters* **99**, 093901 (2007).
- [13] W. H. Zurek, *Reviews of Modern Physics* **75**, 715 (2003).
- [14] G. D. Cole, I. Wilson-Rae, K. Werbach, M. R. Vanner, and M. Aspelmeyer, *Nature Communications* **2**, 231 (2011).
- [15] I. Wilson-Rae, R. A. Barton, S. S. Verbridge, D. R. Southworth, B. Ilic, H. G. Craighead, and J. M. Parpia, *Physical Review Letters* **106**, 047205 (2011).
- [16] P. L. Yu, T. P. Purdy, and C. A. Regal, *Physical Review Letters* **108**, 083603 (2012).
- [17] T. P. M. Alegre, A. Safavi-Naeini, M. Winger, and O. Painter, *Optics Express* **19**, 5658 (2011).
- [18] P. L. Yu, K. Cicak, N. S. Kampel, Y. Tsaturyan, T. P. Purdy, R. W. Simmonds, and C. A. Regal, *Applied Physics Letters* **104**, 023510 (2014).
- [19] R. A. Norte, Ph.D. thesis, California Institute of Technology (2014).
- [20] E. Serra, A. Borrielli, F. S. Cataliotti, F. Marin, F. Marino, A. Pontin, G. A. Prodi, and M. Bonaldi, *Physical Review A* **86**, 051801 (2012).
- [21] J. Liu, F. A. Torres, Y. Ma, C. Zhao, L. Ju, D. G. Blair, S. Chao, I. Roch-Jeune, R. Flamini, C. Michel, et al., *Applied Optics* **53**, 841 (2014).
- [22] J. A. Haringx, *Philips Technisch Tijdschrift* **1**, 16 (1947).
- [23] G. M. Harry and (for the LIGO Scientific Collaboration), *Classical and Quantum Gravity* **27**, 084006 (2010).
- [24] A. Borrielli, A. Pontin, F. Cataliotti, L. Marconi, F. Marin, F. Marino, G. Pandraud, G. A. Prodi, E. Serra, and M. Bonaldi, *Physical Review Applied* **3**, 054009 (2015).
- [25] S. Thornton and J. Marion, *Classical Dynamics of Particles and Systems* (Thomson Learning, 2004), chap. 3.
- [26] D. Kleckner, B. Pepper, E. Jeffrey, P. Sonin, S. M. Thon, and D. Bouwmeester, *Optics Express* **19**, 19708 (2011).
- [27] Q. P. Unterreithmeier, T. Faust, and J. P. Kotthaus, *Physical Review Letters* **105**, 027205 (2010).
- [28] C. A. Zorman and M. Mehregany, *Springer Handbook of Nanotechnology* (Springer, 2010), chap. 11, 3rd ed.
- [29] F. M. Buters, H. J. Eerkens, K. Heeck, M. J. Weaver, B. Pepper, S. de Man, and D. Bouwmeester, *Physical Review A* **92**, 013811 (2015).
- [30] H. J. Eerkens, F. M. Buters, M. J. Weaver, B. Pepper, G. Welker, K. Heeck, P. Sonin, S. de Man, and D. Bouwmeester, *Optics Express* **23**, 8014 (2015).
- [31] I. Wilson-Rae, *Physical Review B* **77**, 245418 (2008).
- [32] A. A. Clerk, F. Marquardt, and K. Jacobs, *New Journal of Physics* **10**, 095010 (2008).
- [33] B. M. Zwickl, W. E. Shanks, A. M. Jayich, C. Yang, A. C. B. Jayich, J. D. Thompson, and J. G. E. Harris, *Applied Physics Letters* **92**, 103125 (2008).
- [34] M. Leivo and J. Pekola, *Applied Physics Letters* **72**, 1305 (1998).
- [35] H. Ftouni, C. Blanc, D. Tainoff, A. D. Fefferman, M. De-foort, K. J. Lulla, J. Richard, E. Collin, and O. Bourgeois, *Physical Review B* **92**, 125439 (2015).
- [36] If  $\omega \gg \omega_o$ , the transfer function is well approximated as  $T(\omega) = \omega_o^4/\omega^4$ , which falls off at 40 dB per decade and is independent of the outer resonator quality factor.